Transport Properties of an Organic Mott Insulator β'-(BEDT-TTF)$_2$ICl$_2$

N. TAJIMA[1], R. KATO[1] and H. TANIGUCHI[2]

[1] *RIKEN, Hirosawa 2-1, Wako-shi, Saitama 351-0198, Japan*
[2] *Saitama University, Shimo-Ohkubo 225, Saitama, 338-8570, Japan*

PACS 71.20.Rv – Polymers and organic compounds
PACS 72.15.Gd – Galvanomagnetic and other magnetotransport effects
PACS 75.47.-m – Magnetotransport phenomena; materials for magnetotransport

Abstract. - We have investigated the temperature dependence of the Hall coefficient and the resistivity of an organic Mott insulator, β'-(BEDT-TTF)$_2$ICl$_2$ under ambient and hydrostatic pressures up to 2 GPa. The charge gap, Δ, the effective mass, m^*, and the scattering lifetime of carriers on Mott Hubbard bands were evaluated by analyzing these transport properties. We found that m^* and Δ are written approximately as $1/m^* \propto (1 - \Delta/U_{\rm eff})$ in the low-pressure region and obtained the value of the effective on-site Coulomb energy, $U_{\rm eff}$, of $\sim$445 meV. Moreover, we reveal that the effective scattering lifetime is proportional to the average distance between carriers in the two-dimensional plane, which suggests the existence of a scattering process attributable to carrier-carrier umklapp scattering in the Mott insulating state.

For many years, both organic and inorganic materials with strongly correlated electron systems have fascinated physicists as a source of exotic superconductors and/or new physics. In those materials, on-site Coulomb energy is one of the most important physical quantities. Usually, on-site Coulomb energy is theoretically determined on the basis of x-ray crystallographic data. In the strongly correlated systems, on the other hand, it has been determined experimentally from optical spectra studies, but the analysis of those spectra are complicated [1–4]. In this paper, we report that on-site Coulomb energy in the Mott insulating state can be successfully evaluated from a simple analysis of transport properties. Experiments were performed on an organic Mott insulator, β'-(BEDT-TTF)$_2$ICl$_2$ (BEDT-TTF=Bis(ethylene-dithio)tetrathiafulvalene), which exhibits superconductivity with $T_{\rm C}$ = 14.2 K under high pressure [5]. To our knowledge, this is the first example of the evaluation of on-site Coulomb energy from transport properties. The scattering mechanism of carriers is also a critical issue in the Mott insulator. We demonstrate that the scattering process in the present conduction is attributable to carrier-carrier umklapp scattering.

The crystal of β'-(BEDT-TTF)$_2$ICl$_2$ forms a layered structure consisting of conductive layers of BEDT-TTF molecules and insulating layers of ICl_2^- anions [6]. According to band calculations [6], this salt is a quasi-one-dimensional (Q1D) system with a pair of warped open Fermi surfaces. Indeed, the reflectance spectra indicate that this system is Q1D [7]. (In contrast, we reveal here that the transport properties demonstrate the 2D nature of the carrier system.) This material, however, behaves as a semiconductor (insulator). This state is not due to nesting of the 1D Fermi surface. The structure has a close-packed arrangement of BEDT-TTF molecular dimers. On each dimer, one unpaired electron is localized as a

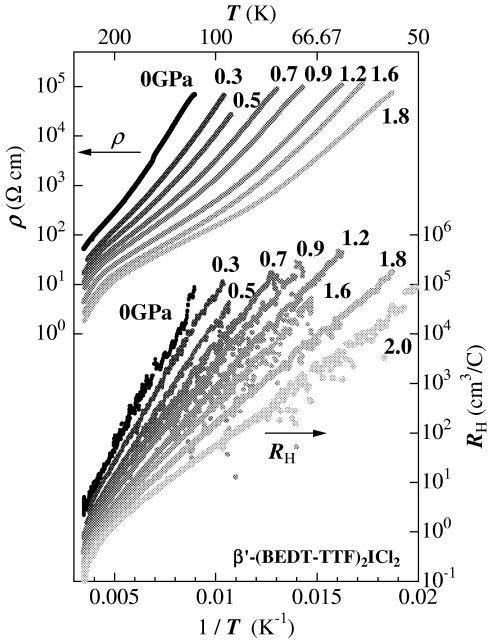

Fig. 1: Temperature dependence of resistivity and Hall coefficient for β'-(BEDT-TTF)$_2$ICl$_2$ under several pressures.

result of the on-dimer Coulomb repulsion. Thus, this material is a Mott insulator. The spin system undergoes a antiferromagnetic transition at 22 K [8–10].

This material is relatively insensitive to pressure. For conventional organic conductors, the piston-cylinder-type pressure cell is widely used as a pressurizing system in the range of 0-2.0 GPa. This pressure range, however, is not sufficient to metalize the present insulator. In 2003, Taniguchi *et al.* performed electrical resistivity measurements with a cubic anvil press, which enables resistivity measurements under high pressures of 2.0-10.0 GPa [5, 11]. Consequently, superconductivity with $T_C = 14.2$ K, which is the highest recorded for organic materials, was realized at an extremely high hydrostatic pressure of around 8 GPa [5]. According to the theoretical works by Kontani [12] and Kino *et al.*, [13] superconductivity with d_{xy}- symmetry is realized next to the antiferromagnetic phase.

In order to understand the superconductivity adjacent to the Mott insulator phase, it is essential to study transport phenomena in the Mott insulating state. Accordingly, β'-(BEDT-TTF)$_2$ICl$_2$, which is the most typical Mott insulator among the known organic conductors, is suitable for this study. To clarify the nature of carriers on Mott Hubbard bands, an investigation of the Hall effect is essential.

The resistivity and the Hall coefficient were measured as a function of temperature between 50 K and 300 K. Experiments were performed as follows. A sample attached with six electrical leads was encased in a Teflon capsule filled with a pressure medium (Idemitsu DN-oil 7373). The capsule was set in a clamp-type pressure cell made of MP35N hard alloy. Resistance was measured by a conventional DC method with six probes. Electrical current was applied in the direction of the second conducting axis (crystallographic c-axis). Magnetic field below 5 T was applied in the direction normal to the conducting plane. In this magnetic field region, the Hall coefficient was field independent.

Figure 1 shows the temperature dependence of resistivity, $\rho(T)$, and Hall coefficient, $R_H(T)$, under several pressures. At ambient pressure (0 GPa), both $\rho(T)$ and $R_H(T)$ roughly obey an activation law. Resistivity increases by about 3 orders of magnitude from about 10^2 Ωcm at 300 K to about 10^5 Ωcm at 90 K. In this region, the Hall coefficient is positive

and therefore the dominant carriers are to be holes. The Hall coefficient increases by more than 4 orders of magnitude from about 3 cm^3/C to about 10^5 cm^3/C. When pressure was applied up to 1.8 GPa, both resistivity and Hall coefficient decreased. At 90 K, for example, they decreased from $\rho \sim 10^5$ Ωcm and $R_{\rm H} \sim 10^5$ cm^3/C at 0 GPa to $\rho \sim 10^2$ Ωcm and $R_{\rm H} \sim 50$ cm^3/C at 1.8 GPa. Over the whole pressure range, the Hall coefficient depends exponentially on temperature below 200 K.

This behavior seems to be the same as that of conventional semiconductors. Detailed examination of resistivity data, however, suggests that resistivity does not obey an activation law above 0.5 GPa. The temperature dependence of resistivity is clearly weaker than that of the Hall coefficient over the whole pressure range. This behavior suggests that the scattering process of carriers in the present Mott insulating state is different from that in conventional semiconductors.

To clarify the nature of carriers in this system, we deduce the temperature dependence of carrier density and carrier mobility from the data of $\rho(T)$ and $R_{\rm H}(T)$. According to ref. [14], the corrected Hall coefficient for Q1D "metal"is given by $R_{\rm H} = 1/n|e| \times k_{\rm F}a/\tan(k_{\rm F}a)$. In this case, it is difficult to extract the carrier density from the Hall coefficient. However, the present system is not a metal but a semiconductor (or insulator) with finite effective masses. We here analyze the data of $\rho(T)$ and $R_{\rm H}(T)$ in the present system as a 2D semiconductor for the following reasons. One is that the strong temperature dependence of the resistivity and the Hall coefficient obeys the activation law (fig. 1). The other is the small anisotropy of conductivity, σ_a/σ_b, in the conducting plane. The ratio σ_a/σ_b is less than 10 at ambient pressure. Consequently, the analysis of this system as a (anisotropic-)2D semiconductor system is suitable. Then, the carrier density, $n_{\rm eff}$, is calculated using the Hall coefficient as $R_{\rm H} = 1/n_{\rm eff}e$ on the basis of the single carrier (hole) picture[1]. Note that a simple calculation of the resistivity tensor for an anisotropic-2D system indicates that the component of Hall resistivity is independent of effective mass. Effective mobility, $\mu_{\rm eff}$, on the other hand, is determined using the relation $\rho = 1/(n_{\rm eff}e\mu_{\rm eff})$.

First, let us discuss the temperature dependence of effective carrier density. In a strictly 2D semiconductor with an isotropic energy band and a finite charge gap, Δ, the temperature dependence of the carrier density is expressed as

$$n(T) \propto T\exp(-\frac{\Delta}{2k_{\rm B}T}). \tag{1}$$

From this equation, we obtain

$$\ln(n(T)/T) = -\frac{\Delta}{2k_{\rm B}}\frac{1}{T} + \alpha. \tag{2}$$

Figure 2 shows plots of $\ln(n_{\rm eff}/T)$ vs $1/T$. The charge gap between upper and lower Mott Hubbard bands is estimated from the slope, ξ, ($\Delta = -2k_{\rm B}\xi$). At ambient pressure, the charge gap is estimated to be approximately 280 meV. With increasing pressure up to 2.0 GPa, it monotonically decreases to approximately 120 meV, as shown in the inset of fig. 3. The temperature dependence of effective carrier density also contains information on the effective mass of carriers. In eq. (2), constant α is given by $\alpha = \ln(k_{\rm B}D_{\rm MH}) = \ln(k_{\rm B}m^*/\pi\hbar^2 c)$, where $D_{\rm MH}$ is the density of states and $c \sim 1.3$ nm is the lattice constant along the direction normal to the conducting plane. The effective mass is estimated to be about 6 m_0 from the equation $\alpha = \ln(n/T)$ for $1/T \to 0$ at ambient pressure, where m_0 is the free electron mass. This value decreases to about 2.8 m_0 at 2.0 GPa (inset of fig. 3).

The important is that inverse effective mass linearly decreases in the high charge gap region above 150 meV, as shown in fig. 3. This can be explained on the basis of a few

[1]In this Mott insulator, one hole is localized at a dimer with S=1/2 spin by the correlation. Therefore, the thermally activated carrier should be the hole. The band calculation with no Coulomb interaction shows also a half-filled hole band.

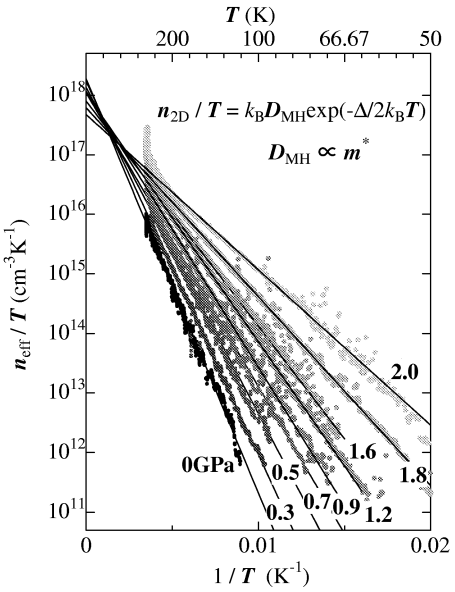

Fig. 2: Temperature dependence of effective carrier density estimated from Hall coefficient. Carrier density in a 2D semiconductor is expressed as $\ln(n(T)/T) = -\frac{\Delta}{2k_B}\frac{1}{T} + \alpha$, where $\alpha = \ln(k_B D_{MH}) = \ln(m^*/\pi\hbar^2 c)$. Fitting the curve to the data below 200 K, we obtain charge gap, Δ, and effective mass, m^*, under several pressures.

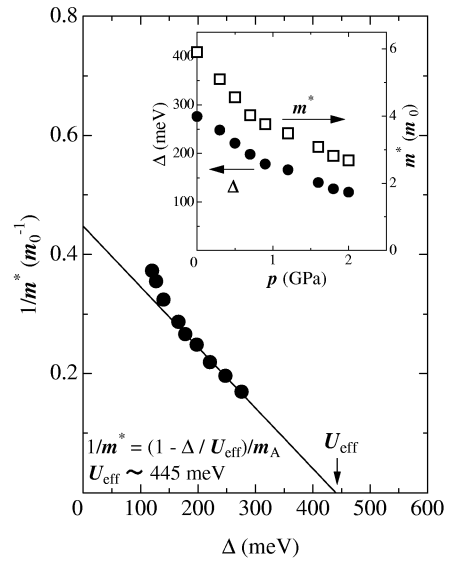

Fig. 3: Inverse effective mass vs charge gap curve. Inset shows pressure dependence of charge gap and effective mass. Using the most simple approximation, we obtain the relationship written as $1/m^* \propto (1 - \Delta/U_{\rm eff})$. Fitting the curve to the data above 150 meV (solid line), the effective on-site Coulomb energy $U_{\rm eff}$ is estimated to be about 445 meV.

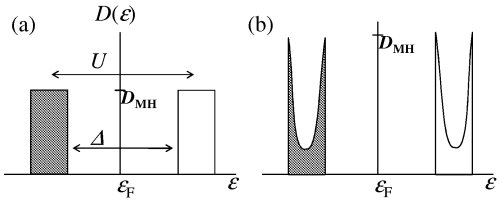

Fig. 4: (a) Schematic illustration of density of states in the 2D Mott insulator (upper and lower Mott Hubbard bands). Δ is charge gap and U is on-site Coulomb energy. (b) Density of states in the present system, predicted from our results, the band calculation [6], and the reflectance spectra [7].

assumptions. The first assumption is that the Fermi level does not move with temperature. Second, on-site Coulomb energy, U, can be regarded as the energy difference between the centers of upper and lower Mott Hubbard bands, and these bands are symmetrical to each other against the Fermi level (fig. 4(a)). Third, we assume that on-site Coulomb energy is unchanged by pressure. Under these assumptions, the total number of holes, $N_{\rm h}$, per unit cell is expressed as

$$N_{\rm h} = \int D(\varepsilon){\rm d}\varepsilon = D_{\rm MH}W, \tag{3}$$

where $W = U - \Delta$ is the energy width of the lower Mott Hubbard band. In the present system, $N_{\rm h} = D_{\rm MH}W$ should be constant ($N_{\rm h} = 1$ hole per unit cell). Thus, inverse effective mass, $1/m^*$, is expressed as

$$\frac{1}{m^*} = \frac{U}{\pi\hbar^2 c N_{\rm h}}(1 - \frac{\Delta}{U}) = \frac{1}{m_A}(1 - \frac{\Delta}{U}). \tag{4}$$

We call the on-site Coulomb energy estimated from this relation for $1/m^* \to 0$, the effective on-site Coulomb energy, $U_{\rm eff}$. The best fit of $1/m^*$ in the charge gap region above 150 meV (in the pressure region below 1.2 GPa) gives $U_{\rm eff} \sim 445$ meV. This value is consistent with 550 meV, obtained by band structure calculation, within a factor of 1.5 [15]. Note that this on-site Coulomb energy is that on the dimer, will be affected by pressure. In β'-Et$_2$Me$_2$P[Pd(dmit)$_2$]$_2$ (dmit = 1,3-dithiole-2-thione-4,5-dithiolate), for example, the pressure dependence of on-site Coulomb energy on a dimer has been estimated; it increases by about 10 % in the range of 0-0.8 GPa at room temperature [16]. Therefore, $U_{\rm eff}$ estimated from the Δ vs $1/m^*$ curve would include an ambiguity of 5-10 %. This ambiguity, however, is negligible compared with the variation of Δ and $1/m^*$ with pressure. Therefore, even though the estimation of $U_{\rm eff}$ from the Δ vs $1/m^*$ curve is oversimplified, it is still a very useful measure. Note that no reliable value of $U_{\rm eff}$ of this material has been reported so far because it is very difficult to determine experimentally.

Next we check the value of $N_{\rm h}$. $N_{\rm h}$ should be 1 hole per unit cell for the present system. However, it is calculated to be about 4 holes per unit cell from the equation $1/m^* = 1/m_A$ for $\Delta \to 0$. Note that the data include errors up to a factor of 2 that arises, for instance, from the difficulty in measuring sample dimensions accurately. The factor of 4, however, is larger than this ambiguity. This high value of $N_{\rm h}$ indicates that the system deviates from the strictly 2D semiconductor toward the Q1D system (fig. 4(b)). Accordingly, the density of states in the present system should be modified, as shown in fig. 4(b), such that $N_{\rm h}$ becomes 1 hole per unit cell. Holes on the band edge dominate the conduction of this system. In this case, the effective mass should be expressed as $m^* = \sqrt{m_a m_b}$, where m_a and m_b are associated with the anisotropy of the effective mass in the 2D conducting plane. At room temperature and ambient pressure, for example, the ratio of m_b/m_a is expected

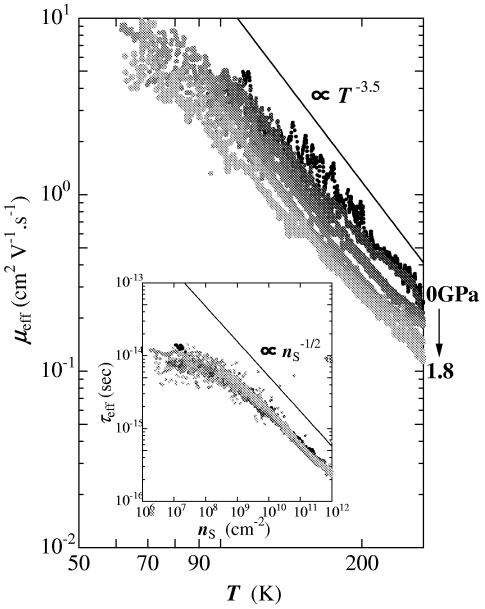

Fig. 5: Temperature dependence of effective mobility, $\mu_{\rm eff}$, for pressures up to 1.8 GPa. Inset shows effective scattering time, $\tau_{\rm eff}$, vs the effective carrier density per layer, $n_{\rm S}$.

to be 5 - 10 from the anisotropy of the conductivity $\sigma_a/\sigma_b \sim 5$ - 10. On the other hand, $m^* = \sqrt{m_a m_b} \sim 6\ m_0$. Thus, m_a and m_b are calculated to be 1.9 - 2.6 m_0 and 13 - 19 m_0 at ambient pressure.

Examining the data in fig. 3 in more detail, we find that the $1/m^*$ vs Δ curve becomes steeper below 150 meV. In this region, the inverse effective mass deviates from the $1/m^* = 1/m_A(1 - \Delta/U)$ curve and obeys the $1/m^* \propto 1/\Delta$ law. This is not due to the variation of lattice constant c with pressure. In α-(BEDT-TTF)$_2$I$_3$, for example, this variation from 0 to 1.8 GPa is only 3 % [17]. The behavior of $1/m^* \propto 1/\Delta$, on the other hand, is commonly observed in narrow gap semiconductors. The interaction between the upper and lower bands, which is a result of the narrowing of the charge gap, tends to induce a lighter mass [18].

The most interesting issue in this system is the scattering process of carriers. The effective carrier mobility of the present system manifests itself in two characteristic features, as shown in fig. 5. One is the temperature dependence. At ambient pressure, effective carrier mobility increases by about 20 times from $\mu_{\rm eff} \sim 0.2$ cm^2/Vs at 300 K to $\mu_{\rm eff} \sim 4$ cm^2/Vs at 100 K. This indicates the power-law-type temperature dependence $\mu_{\rm eff} \propto T^A$, with $A \simeq -3.5$. This temperature dependence is peculiar. In metals with strongly correlated electrons, it is well known that $A = -2$ at low temperature. In conventional semiconductors, on the other hand, the temperature dependence of carrier mobility is proportional to $T^{-1.5}$, which is attributed to acoustic phonon scattering. To our knowledge, this is the first finding of a material in which carrier mobility strongly depends on temperature as $\mu \propto T^{-3.5}$. The other feature is the pressure-dependent effective carrier mobility. Effective carrier mobility decreases with increasing pressure, and yet, the effective mass of carriers decreases (inset of fig. 3). At 100 K, for example, it decreases by a factor of about 3 from $\mu_{\rm eff} \sim 4$ cm^2/Vs at ambient pressure to $\mu_{\rm eff} \sim 1.5$ cm^2/Vs at 1.8 GPa. In this pressure range, on the other hand, the effective mass of carriers decreases by a factor of about 2 from 6 m_0 to 3 m_0. This result strongly suggests that the scattering mechanism in the present system is very peculiar because carrier mobility is expressed as $\mu_{\rm eff} = e\tau/m^*$. Since the exponent $A \simeq -3.5$ in $\mu_{\rm eff} \propto T^A$ is almost pressure independent (fig. 5), the scattering process dose not changed with pressure.

In order to discuss the present scattering mechanism, we estimate the effective scattering time, $\tau_{\rm eff} = \mu_{\rm eff} m^*/e$. It is plotted as a function of effective carrier density per layer, $n_{\rm S}$, in the inset of fig. 5. Since each conductive layer of this material is sandwiched by insulating layers, the conducting layer is almost independent. Therefore, the concept "effective carrier density per layer "is valid for the present system. The effective scattering time can be plotted on a single $\tau_{\rm eff}$ vs $n_{\rm S}$ curve in the whole pressure range examined. Significant is that in the region $n_{\rm S} > 10^9$ cm^{-2}, the effective scattering rate, $1/\tau_{\rm eff}$, is proportional to $(n_{\rm S})^{1/2}$. These results strongly suggest that the scattering process in this system is associated with the carrier density per layer, that is, the average distance between carriers in the 2D plane. This is the reason why effective carrier mobility decreases with increasing pressure. We believe that the $T^{-3.5}$-dependent effective carrier mobility originates from the carrier-carrier umklapp scattering in the Mott insulator.

In conclusion, β'-(BEDT-TTF)$_2$ICl$_2$ under ambient pressure was characterized as a Mott insulator with charge gap $\Delta \sim 280$ meV and effective mass $m^* = \sqrt{m_a m_b} \sim 6\ m_0$. Anisotropic effective mass values m_a and m_b in the conducting plane were calculated to be 1.9 - 2.6 m_0 and 13 - 19 m_0, respectively. When pressure was applied, both charge gap and effective mass monotonically decreased. The relationship between charge gap and effective mass is approximately expressed as $1/m^* \propto (1 - \Delta/U_{\rm eff})$ in a wide charge gap region above 150 meV. This indicates that the variation of charge gap in this system is associated with the bandwidth, because the change in on-site Coulomb energy is small in the low pressure region. Effective on-site Coulomb energy was roughly estimated to be $U_{\rm eff} \sim 445$ meV. Thus far, this is the first report showing the effective on-site Coulomb energy was evaluated by transport experiments. This system provides a testing ground for the carrier-carrier umklapp scattering in the Mott insulating state.

This work was supported by Grants-in-Aid for Scientific Research (Nos. 19540387, 18028007 and 16GS0219) from the Ministry of Education, Culture, Sports, Science and Technology, Japan.

REFERENCES

[1] Tanner D. B, Miller J. S., Rice M. J. and Ristko J. J., *Phys. Rev. B*, **21** (1980) 5835.
[2] Higuchi T., Baba D., Takeuchi T., Tsukamoto T., Taguchi Y., Tokura Y., Chainani A. and Shin S., *Phys. Rev. B*, **68** (2003) 104420.
[3] Kézmárki I., Shimizu Y., Mihály G., Tokura Y., Kanoda K. and Saito G., *Phys. Rev. B*, **68** (2003) 104420.
[4] Gössling A., Haverkort M. W., Benomar M., Wu H., Senff D., Möller T., Branden M., Mydosh J. A. and Grüninger M., *Phys. Rev. B*, **77** (2008) 035109.
[5] Taniguchi H., Miyashita M., Uchiyama K., Satoh K., Mori N., Okamoto H., Miyagawa K., Kanoda K., Hedo M. and Uwatoko Y., *J. Phys. Soc. Jpn.*, **72** (2003) 468.
[6] Kobayashi H., Kato R., Kobayashi A., Saito G., Tokumoto M., Anzai H. and Ishiguro T., *Chem. Lett.*, (1986) 89.
[7] Kuroda H., Yakushi K., Tajima H., Ugawa A., Tamura M., Okawa Y., Kobayashi A., Kato R., Kobayashi H. and Saito G., *Synth. Met.*, **27** (1988) A491.
[8] Tokumoto M., Anzai H., Ishiguro T., Saito G., Kobayashi H., Kato R. and Kobayashi A., *Synth. Met.*, **19** (1987) 215.
[9] Yoneyama N., Miyazaki A., Enoki T. and Saito G., *Synth. Met.*, **86** (1997) 2029.
[10] Kanoda K., *J. Phys. Soc. Jpn.*, **75** (2006) 051007.
[11] Môri N., Okayama Y., Takahashi H., Haga Y. and Suzuki T., *Physical Properties of Actinide and Rare Earth Compounds* (JJAP, Tokyo) 1993, p. 182.
[12] Kontani H., *Phys. Rev. B*, **67** (2003) 180503.
[13] Kino H., Kontani H. and Miyazaki T., *J. Phys. Soc. Jpn.*, **73** (2004) 25.
[14] Moser J., Cooper J. R., Jérome D., Alavi B., Brown S. E. and Bechgaard K., *Phys. Rev. Lett.*, **84** (2000) 2674.
[15] Ishiguro T., Yamaji K. and Saito G., *Organic Superconductors* (Springer) 1998.

[16] Yamaura J., Nakao A. and Kato R., *J. Phys. Soc. Jpn.*, **73** (2004) 976.
[17] Tamura I., Kobayashi H. and Kobayashi A., *J. Phys. Chem. Solids*, **63** (2002) 1255.
[18] Kittel C., *Quantum Theory of Solids, 2nd ed.* (Wiley, New York) 1986.